DRD1 plans on gaseous detectors for PID

F. Grancagnolo

INFN – Lecce

ECFA WG3: Topical workshop on calorimetry, PID and photodetectors

CERN, 3–4 May 2023

Strategy

To evaluate the **requirements of PID**, one must provide examples of relevant physics processes

Strategy

To evaluate the **requirements of PID**, one must provide examples of relevant physics processes:

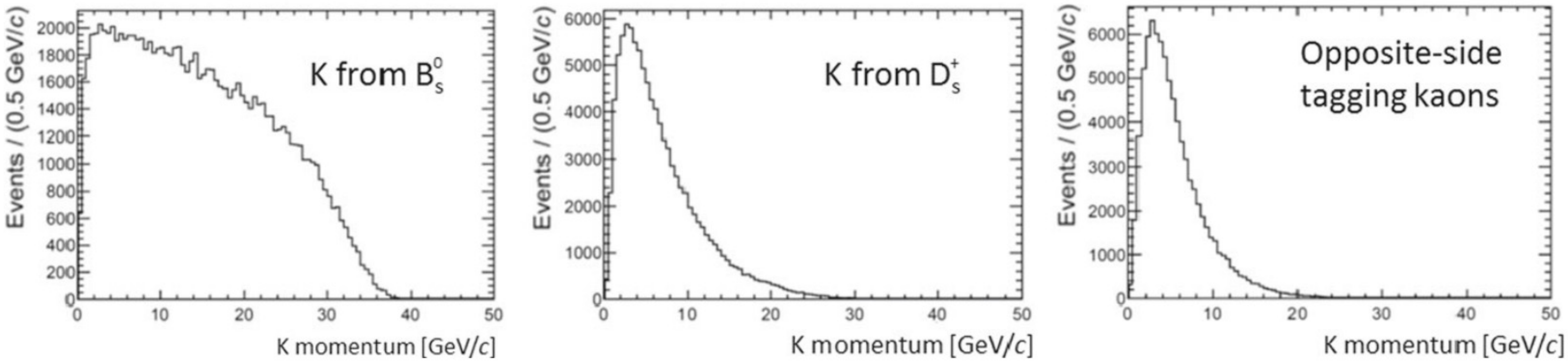

Momentum spectra for kaons occurring in Z^0 events containing a $B_s^0 \to D_s^{\pm} K^{\mp}$ decay.

From: Guy Wilkinson - *Particle identification at FCC-ee* - Eur. Phys. J. Plus (2021) 136:835 - https://doi.org/10.1140/epjp/s13360-021-01810-4

Strategy

To evaluate the **requirements of PID**, one must provide examples of relevant physics processes

To estimate the **performance** of a particular **PID system**, one may consider improvement factors with respect to **no-PID** (efficiency?) vs purity of PID for benchmark channels

Strategy

To evaluate the **requirements of PID**, one must provide examples of relevant physics processes

To estimate the **performance** of a particular **PID system**, one may consider improvement factors with respect to **no-PID** (efficiency?) vs purity of PID for benchmark channels

Example: $B_s^0 \to D_s^{\mp} K^{\pm}$

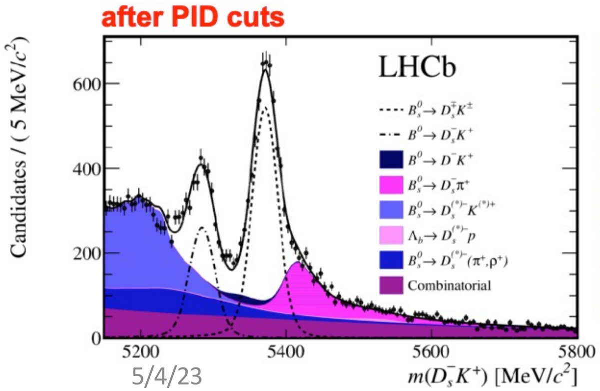

[LHCb, JHEP 05 (2015) 019]

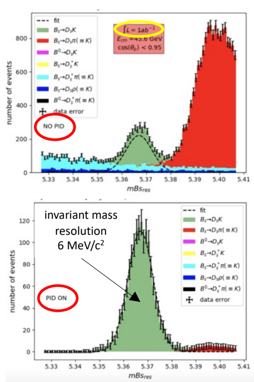

PID at 5% and TOF at 100 ps

R. Aleksan , L. Oliver and E. Perez – arXiv:2107.02002v1 [hep-ph] 5 Jul 2021

Example: 2-prongs *B-decays*

LHCb - JHEP 10 (2012) 037

Without PId

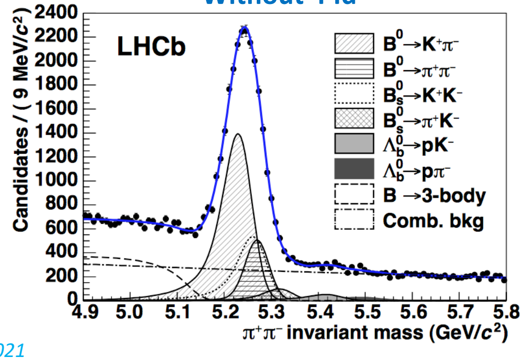

with PId

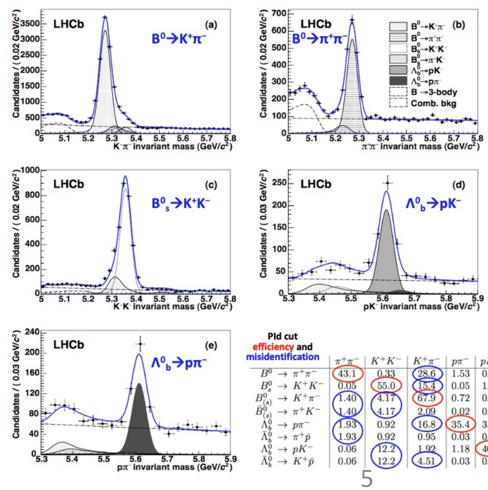

PId cut efficiency and misidentification

	$\pi^+\pi^-$	K^+K^-	$K^+\pi^-$	$p\pi^-$	pK^-
$B^0 \to \pi^+\pi^-$	43.1	0.33	28.6	1.53	0.13
$B_s^0 \to K^+K^-$	0.05	55.0	15.4	0.05	1.63
$B_{(s)}^0 \to K^+\pi^-$	1.40	4.17	67.9	0.72	0.06
$\bar{B}_{(s)}^0 \to \pi^+K^-$	1.40	4.17	2.09	0.02	0.85
$\Lambda_b^0 \to p\pi^-$	1.93	0.92	16.8	35.4	3.16
$\bar{\Lambda}_b^0 \to \pi^+\bar{p}$	1.93	0.92	0.95	0.03	0.18
$\Lambda_b^0 \to pK^-$	0.06	12.2	1.92	1.18	40.2
$\bar{\Lambda}_b^0 \to K^+\bar{p}$	0.06	12.2	4.51	0.03	0.18

Strategy

To evaluate the **requirements of PID**, one must provide examples of relevant physics processes

To estimate the **performance** of a particular **PID system**, one may consider improvement factors with respect to **no-PID** (efficiency?) vs purity of PID for benchmark channels

Consider **all possible options**

Particle Identification technologies

$$\frac{m^2}{p^2} = \frac{1}{\gamma^2 - 1} = \frac{1-\beta^2}{\beta^2}$$

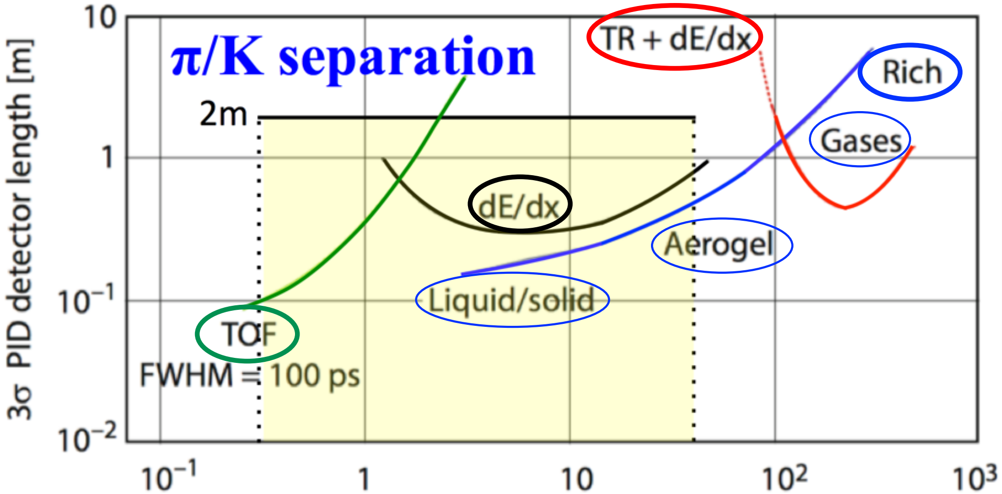

Forty R. and Ullaland O.
https://doi.org/10.1007/978-3-030-35318-6_7
(adapted from B. Dolgoshein NIM A433 (1999) 533)

dE/dx

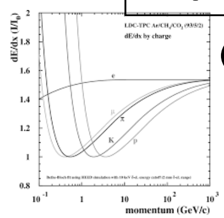

$$-\frac{dE}{dx} = Kz^2\frac{Z}{A}\frac{1}{\beta^2}\left[\ln\frac{2m_ec^2\beta^2\gamma^2T_{max}}{I^2} - \beta^2 - \frac{\delta(\beta\gamma)}{2}\right]$$

$$T_{max} = \frac{2m_ec^2\beta^2\gamma^2}{1+\frac{2\gamma m_e}{M}+\left(\frac{m_e}{M}\right)^2}$$

$$N_{cluster} = \int_0^L \frac{1}{w(x)}\frac{dE}{dx}dx$$

$dN_{cluster}/dx$

$$\Delta t = \frac{L}{c}\left(\frac{1}{\beta_1}-\frac{1}{\beta_2}\right) = \frac{L}{c}\left(\sqrt{1+m_1^2c^2/p^2}-\sqrt{1+m_2^2c^2/p^2}\right) \approx \frac{Lc}{2p^2}\left(m_1^2-m_2^2\right)$$

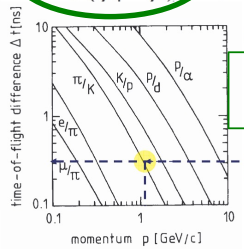

Δt for L = 1 m path length

TOF

σ_t = 300 ps
π/K separation up to 1 GeV/c

$$\cos\theta_c = \frac{1}{n\beta}$$

Rich

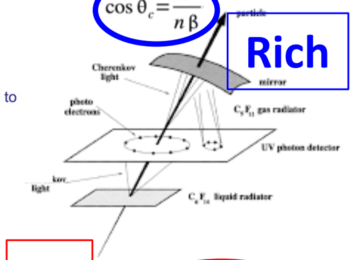

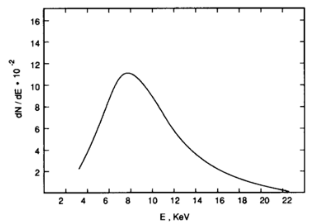

TR

$$W = \frac{1}{3}\alpha\hbar\omega_p\gamma$$

$$\omega_p = \sqrt{\frac{N_e e^2}{\epsilon_0 m_e}} \qquad \hbar\omega_p = 20\,eV$$

Strategy

To evaluate the **requirements of PID**, one must provide examples of relevant physics processes

To estimate the **performance** of a particular **PID system**, one may consider improvement factors (efficiency?) vs purity of PID for benchmark channels

Consider **all possible options**

Concentrate attention on **dE/dx** and **Cluster Counting** in **gaseous detectors**

PID with dE/dx: the task

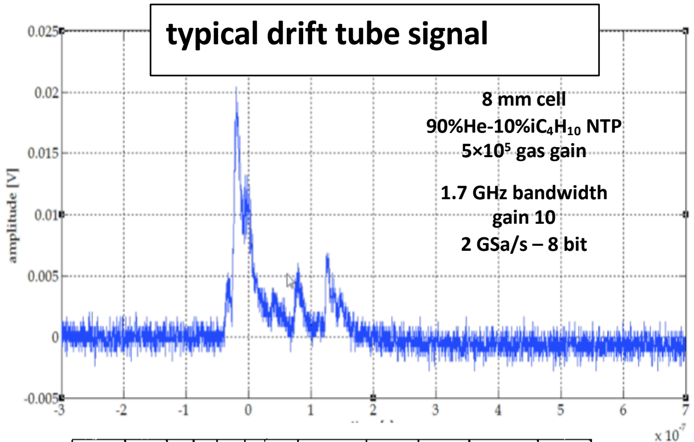

By definition, **the integral** of the drift signal is proportional to the **total number of electrons** liberated and collected in the ionization process which, in turn, is proportional to the **energy lost** by the charged particle crossing the layer **x** of gas **(-dE/dx)**.
Knowing the dependence of dE/dx from the velocity **β** of the crossing particle, given **p**, one can identify the particle **mass**.

Also, the **theory model description of the energy loss mechanism** needs to be accurate **at 1% level**

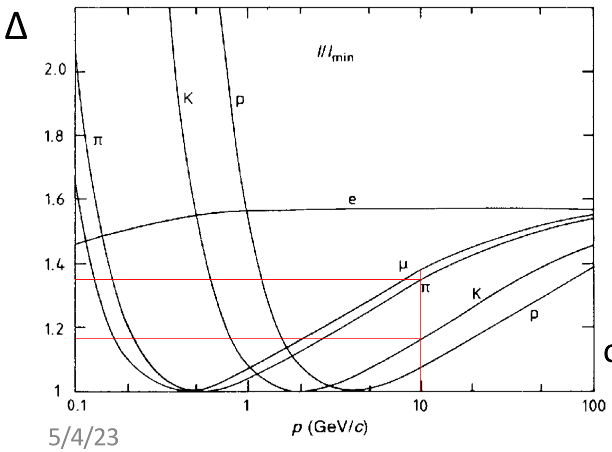

In the relativistic rise region:
[Δ(π) – Δ(K)] / Δ(π) ≈
≈ 10-15%
π/K separation
requires
resolutions δΔ/Δ
of **better than a few %**

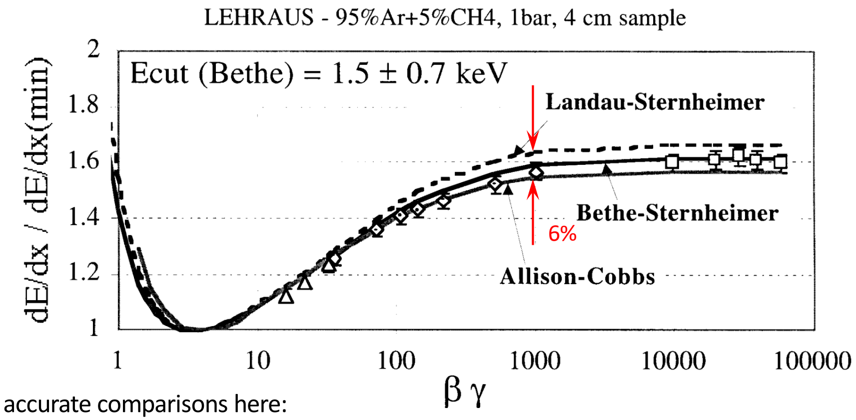

more accurate comparisons here:
J. Va'vra *Particle Identification Methods in High Energy Physics,* **SLAC-PUB-8356, Jan. 2000**

PID with dE/dx: the straggling function

Definitions and iterative application of **convolution integral**

$d\sigma(E,\beta)/dE$ collision cross section for an energy transfer **E** by a particle of velocity **β**
$\lambda = \lambda(\beta) = 1/(n_e\sigma)$ mean free path between collisions (**n_e** = linear density of electrons)
$N_c = x/\lambda$ mean number of collisions over a length **x**

$\mathcal{F}_{(1)}(E) = 1/\sigma \, d\sigma(E,\beta)/dE = n_e\lambda \, d\sigma(E,\beta)/dE$
probability to transfer energy **E** in a single collision

$\mathcal{F}_{(k)}(\Delta) = \int_0^{\Delta} \mathcal{F}_{(1)}(E)\, \mathcal{F}_{(k-1)}(\Delta - E)\, dE$ probability to transfer energy **Δ** in **k** collisions
k-fold convolution of $\mathcal{F}_{(1)}(E)$

$\mathcal{P}(k, N_c) = N_c^k/k! \exp(-N_c)$ probability of **k** collisions with mean **N_c** (Poisson)

$f(\Delta,x) = \sum_{k=0}^{\infty} \mathcal{P}(k, N_c)\, \mathcal{F}_{(k)}(\Delta)$ probability density function for energy loss **Δ** over **x**
(straggling function)

for a rigorous treatment see:
H. Bichsel *A method to improve tracking and particle identification in TPCs and silicon detectors* **NIM A562 (2006) 154**

straggling function

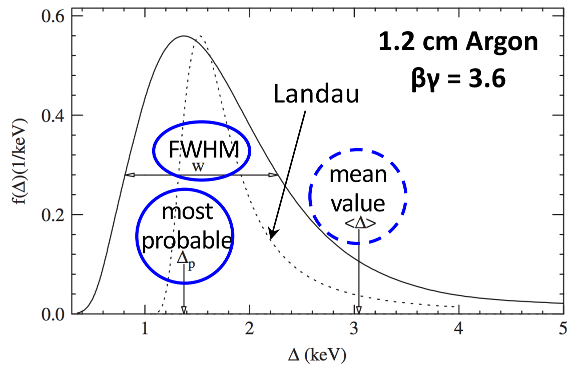

Fig. 1. The straggling function $f(\Delta)$ for particles with $\beta\gamma = 3.6$ traversing 1.2 cm of Ar gas is given by the solid line. It extends beyond $E_{max} \sim 2mc^2\beta^2\gamma^2 = 13$ MeV. The original Landau function [2,3] is given by the dotted line. Parameters describing $f(\Delta)$ are the most probable energy loss $\Delta_p(x;\beta\gamma)$, i.e. the position of the maximum of the straggling function, at 1371 eV, and the full-width-at-half-maximum (FWHM) $w(x;\beta\gamma) = 1463$ eV. The mean energy loss is $\langle\Delta\rangle = 3044$ eV.

parameters describing the
straggling function:
most probable energy loss **$\Delta_p(x,\beta\gamma)$**
and FWHM **$W(x,\beta\gamma)$**

PID with dE/dx: maximum likelihood measurement

- There exist several different approaches to calculate the energy loss distribution (**the straggling function**) besides the **convolution method** (iterative application of convolution integral):
  Laplace transform method*, **Monte Carlo** method**, **empirical fit to data*****
  and a plethora of different models based on different parameterization of the collision cross section **σ** with *ad-hoc* corrections

  *L. Landau, J. Phys. USSR 8, 201 (1944), **Cobb et al., Nucl. Instr. Meth. 133, 315 (1976),
  ***Blum, Riegler, Rolandi, Springer-Verlag 2008 - doi: 10.1007/978-3-540-76684-1 10

- The energy loss distribution (straggling function) f **(Δ)** for a single sample is made of **a broad peak** due to low energy transfer (**soft**) **collisions** with the gas molecules and **a long tail** due to large energy transfer (**hard**) **collisions** which cause the release of **more than one electron** and/or **δ rays**

- Typical **FWHM** of the energy loss distribution is in the range of **60-100%** Δ_p (very slowly dependent from βγ – except for very small sample lengths), which makes necessary to measure many samples (**n**) along the ionizing track in order to get a good enough estimate of the energy loss.

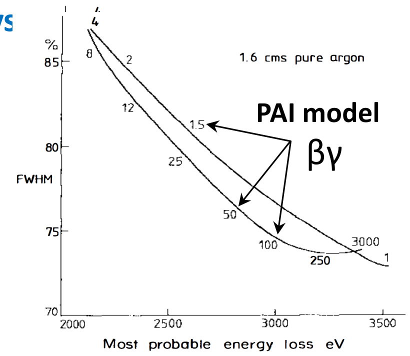

From: W. Allison and J. Cobb
. Rev. Nucl. Part. Sci. 1980. 30: 253-98

- With the assumption that the shape of the straggling function doesn't depend on βγ, one can construct a **likelihood function**:

$$\mathcal{L}(\lambda) = \prod_{i=1}^{n} f(\Delta_i/\lambda).$$

The λ_0 (with its error $\delta(\lambda_0)$) which maximizes $\mathcal{L}(\lambda)$ is normally distributed and represents **the measured value of the most probable energy loss by the track under scrutiny**.
The mass assignment may then be calculated by comparing the expected ionization with λ_0 and $\delta(\lambda_0)$ using **normal error statistics**.

PID with dE/dx: truncated mean measurement

- A much simpler and more robust procedure for obtaining analogous results is the method of **truncated mean**.
- It consists in cutting out a fraction **(1−η)•n** of the largest **Δ_i** samples and extending the arithmetic mean to the remaining **η•n** values (**m** is the closest integer to η•n):

$$\langle\Delta\rangle_\eta = 1/m \sum_{j=1}^{m} \Delta_j \qquad \Delta_j \le \Delta_{j+1} \quad \text{for } j = 1, \ldots, n-1$$

- It can be shown that the range of values of **η** which minimizes the relative fluctuations of **$\langle\Delta\rangle_\eta$** for **Argon** is **between 0.4 and 0.7** (**0.8 for Helium**). Moreover, the **$\langle\Delta\rangle_\eta$** distribution behaves like a **gaussian distribution.**
- This is equivalent to the maximum likelihood method with: $\langle\Delta\rangle_\eta \cong \lambda_0$ and $\sigma(\langle\Delta\rangle_\eta) \cong \delta(\lambda_0)$

PID with dE/dx: truncated mean measurement

- A much simpler and more robust procedure for obtaining analogous results is the method of **truncated mean**.
- It consists in cutting out a fraction **(1−η)·n** of the largest Δ_i samples and extending the arithmetic mean to the remaining **η·n** values (**m** is the closest integer to η·n):

$$<\Delta>_\eta = 1/m \sum_{j=1}^{m} \Delta_j \qquad \Delta_j \leq \Delta_{j+1} \quad \text{for } j = 1, \ldots, n-1$$

- It can be shown that the range of values of **η** which minimizes the relative fluctuations of $<\Delta>_\eta$ for **Argon** is **between 0.4 and 0.7** (**0.8 for Helium**). Moreover, the $<\Delta>_\eta$ distribution behaves like a **gaussian distribution.**
- This is equivalent to the maximum likelihood method with: $<\Delta>_\eta \cong \lambda_0$ and $\sigma(<\Delta>_\eta) \cong \delta(\lambda_0)$

- **ALTERNATIVES** to arithmetic mean**?**

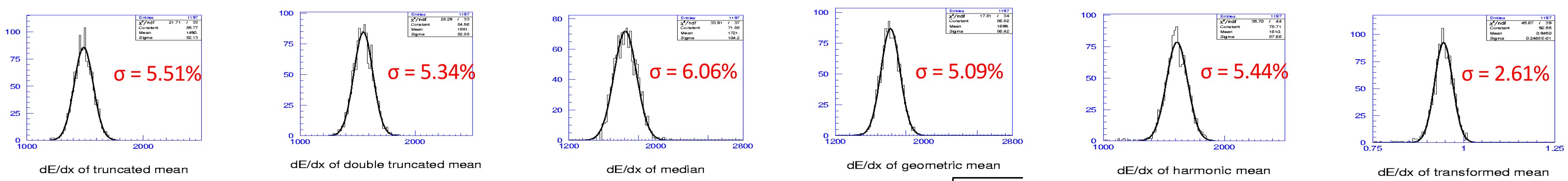

TM 70%

2TM 5-75%

$$<\Delta>_g = \sqrt[n]{\prod_{i=1}^{n} \Delta_i}$$

$$<\Delta>_h = \frac{n}{\sum_{i=1}^{n} 1/\Delta_i}$$

$$<\Delta>_t = \left(\sum_{i=1}^{n} \frac{1}{\sqrt{\Delta_i}} \right)^{-1}$$

(BESIII data) From: **M. Hauschild** *Progress in dE/dx techniques used for particle identification* **NIM A379(1996) 436**

PID with dE/dx: particle separation power

- The relevant quantity for discriminating between two different particle of masses **1** and **2** of momentum **p**, rather than λ_0 and $\delta(\lambda_0)$ for each of them, is:

$$D_{12}(p) = \frac{|\lambda_{0,1}(p) - \lambda_{0,2}(p)|}{[\sigma(\lambda_{0,1}) + \sigma(\lambda_{0,2})]/2}$$

(separation measured in numbers of sigma $\sigma(\lambda_0) = \delta(\lambda_0)/\lambda_0$)

ALEPH TPC

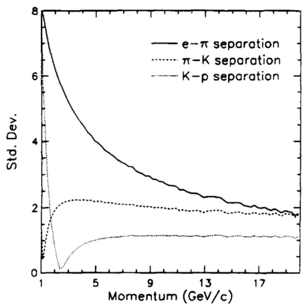

two-sided truncated mean: discard lowest 8% and largest 40%

$$\frac{\sigma_{dE/dx}}{(dE/dx)} = 4.5\%$$

OPAL Drift Chamber (4 bar)

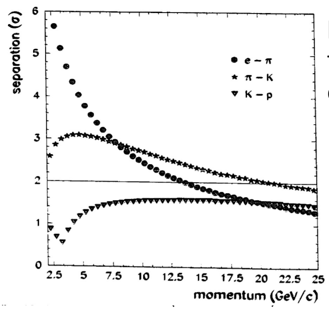

hit quality cuts and truncated mean: discard largest 30%

$$\frac{\sigma_{dE/dx}}{(dE/dx)} = $$

3.1% (dimuons)

3.8% (m.i.p.)

- The number of ionization acts follows **Poison distribution** (≈10/cm/bar for He based, ≈30/cm/bar for Ar based gases)
- The number of electrons generated in each ionization act (**cluster size**) is subject to large fluctuations
- The accuracy of the ionization measurement depends on the mean free path between ionizing collisions $\boldsymbol{\lambda = 1/(n_e\sigma)}$ (i.e., on the collision cross section $\boldsymbol{\sigma}$ and on the electron number density $\boldsymbol{n_e}$), therefore, on
  - the **gas** mixture;
  - the **sample length x** and its density, or the **gas pressure p** through their product **xp**;
  - the number of samples **n**, or, equivalently, the total length of the track **L = nx**.
- **Empirical parameterization of resolution**

  $\sigma(\lambda_0) = \delta(\lambda_0)/\lambda_0$ ([%] xp in [cm bar]):

$$\boldsymbol{\sigma(\lambda_0) = 41\, n^{-0.46} (xp)^{-0.32}\ [\%]} \quad \textbf{for Argon}$$

based on max. likel., −0.46 → −0.43 with trunc. mean
(Allison-Cobb *Walenta)*

PID with dE/dx: general comments

- ✧ Methodology dating back to late ‘70s. Very little progress in performance since then.

PID with dE/dx: general comments

✧ Methodology dating back to late ‘70s. Very little progress in performance since then.

Detector	Accelerator	Type	Size (Ø x L)	B (T)	Gas Mixture	Pressure (bar)	Number of samples	Sampling length (mm)	Effective detector length (bar * m)	dE/dx resolution (%) isolated tracks	dE/dx resolution (%) dense tracks	Truncation (%)	Reference
ALEPH	LEP	TPC	3.6 m x 4.4 m	1.5	Ar/CH_4 (91/9)	1	338	4	1.35	4.5		8-60	D. Buskulic et al., NIM A 360 (1995) 481
ALICE	LHC	TPC	5.0 m x 5.0 m	0.5	Ne/CO_2 (90/10)	1	159	7.5, 10, 15	1.60	4.5	(5.0)	0-70	W. Yu, NIM A 706 (2013) 55, J. Alme et al., NIM A 622 (2010) 316
ARGUS	DORIS	drift cells	1.7 m x 2 m	0.8	C_3H_8/Methylal	1	36	18	0.65	4.1	(4.4)	10-70	Y. Oku, PhD Thesis, Univ. of Lund (1985), LUNFD6/(NFFL-7024)/
BaBar	PEP-II	drift cells	1.6 m x 2.8 m	1.5	$He/i\text{-}C_4H_{10}$ (80/20)	1	40	12	0.48	7.5		0-80	B. Aubert et al., NIM A 479 (2002) 1-116
BELLE	KEK-B	drift cells	1.9 m x 2.2 m	1.5	He/C_2H_6 (50/50)	1	47	16	0.75	5.5	(7.0)	0-80	E. Nakano, NIM A 494 (2002) 402-408
BES	BEPC	jet cells	2.3 m x 2.1 m	0.4	$Ar/CO_2/CH_4$ (89/10/1)	1	54	5	0.27	9.0		0-70	J.Z. Bai et al., NIM A 344 (1994) 319
CDF	TEVATRON	jet cells	2.6 m x 3.2 m	1.5	$Ar/C_2H_6/C_2H_6O$ (49.6/49.6/0.8)	1	32	12	0.38	7.0		?	D. Stuart, private communications
CLEO II	CESR	drift cells	1.9 m x 1.9 m	1.5	Ar/C_2H_6 (50/50)	1	51	14	0.71	6.2	(7.1)	0-50	Y. Kubota et al., NIM A 320 (1992) 66
CLEO III	CESR	drift cells	1.6 m x 1.9 m	1.5	He/C_3H_8 (60/40)	1	47	14	0.66	5.0		0-70	D. Peterson et al., NIM A 478 (2002) 142-146
CRISIS	TEVATRON	jet cells	1 m x 1 m x 3 m	-	Ar/CO_2 (80/20)	1	192	15	2.88	3.2		0-75	W.S. Toothacker et al., NIM A 273 (1988) 97
DELPHI	LEP	TPC	2.4 m x 2.7 m	1.2	Ar/CH_4 (80/20)	1	192	4	0.77	5.7	(6.2)	0-80	P. Abreu et. al., CERN-PPE/95-194, submitted to NIM
D0 FDC	TEVATRON	jet cells	1.2 m x 0.3 m	-	$Ar/CH_4/CO_2$ (93/4/3)	1	32	8	0.26	12.7		0-70	S. Rajagopalan, PhD Thesis, Northwestern University (1992)
H1	HERA	jet cells	1.7 m x 2.2 m	1.13	Ar/C_2H_6 (50/50)	1	56	10	0.56	10.0		---*	I. Abt et al., NIM A 386 (1997) 348-396
JADE	PETRA	jet cells	1.6 m x 2.4 m	0.48	$Ar/CH_4/i\text{-}C_4H_{10}$ (88.7/8.5/2.8)	4	48	10	1.92	6.5	(7.2)	5-70	K. Ambrus, PhD Thesis, Univ. of Heidelberg (1986)
KEDR	VEPP-4M	jet cells	1.1 m x 1.1 m	2.0	DME (100)	1	42	10	0.42	10.0		5-70	S.E. Baru et al., NIM A 323 (1992) 151
KLOE	DAΦNE	drift cells	4 m x 3.3 m	0.6	$He/i\text{-}C_4H_{10}$ (90/10)	1	58	28	1.62	3.5		0-80	A. Andryakov et al., NIM A 409 (1998) 390-394 (prototype)
MARK II	SLC	drift cells	3 m x 2.3 m	0.475	$Ar/CO_2/CH_4$ (89/10/1)	1	72	8.33	0.60	7.0		5-75	A. Bojarski et al., NIM A 283 (1989) 617
NA49	SPS	TPC	.8 m x 3.8 m x 1.3 ı	-	$Ar/CH_4/CO_2$ (90/5/5)	1	90	40	3.60	4.7		10-65	B. Lasiuk, NIM A 409 (1998) 402-406
OBELIX	LEAR	jet cells	1.6 m x 1.4 m	0.5	Ar/C_2H_6 (50/50)	1	40	15	0.60	12.0		0-70	F. Balestra et al., NIM A 323 (1992) 523
OPAL	LEP	jet cells	3.6 m x 4 m	0.435	$Ar/CH_4/i\text{-}C_4H_{10}$ (88.2/9.8/2)	4	159	10	6.36	2.8	(3.2)	0-70	M. Hauschild, NIM A 379 (1996) 436
SLD	SLC	jet cells	2 m x 2 m	0.6	$CO_2/Ar/i\text{-}C_4H_{10}$ (75/21/4)	1	80	6	0.48	7.0		?	M. Hildreth, private communications
STAR	RHIC	TPC	4 m x 4.2 m	0.5	Ar/CH_4 (90/10)	1	45	17.2	0.77	8.0		0-70	M. Anderson et al., NIM A 499 (2003), 659
TOPAZ	TRISTAN	TPC	2.4 m x 2.2 m	1.0	Ar/CH_4 (90/10)	3.5	175	4	2.45	4.4	(4.6)	0-65	M. Iwasaki et al., NIM A 365 (1995) 143
TPC/2γ	PEP	TPC	2 m x 2 m	1.375	Ar/CH_4 (80/20)	8.5	183	4	6.22	3.0		0-65	G. Cowan, PhD Thesis, Lawrence Berkeley Lab. (1988), LBL-24715
ZEUS	HERA	jet cells	1.7 m x 2.4 m	1.43	$Ar/CO_2/C_2H_6$ (90/8/2)	1	72	8	0.58	8.5		?	W. Zeuner, private communications

* = inverse gaussian mean 1/sqrt[(dE/dx)i] used

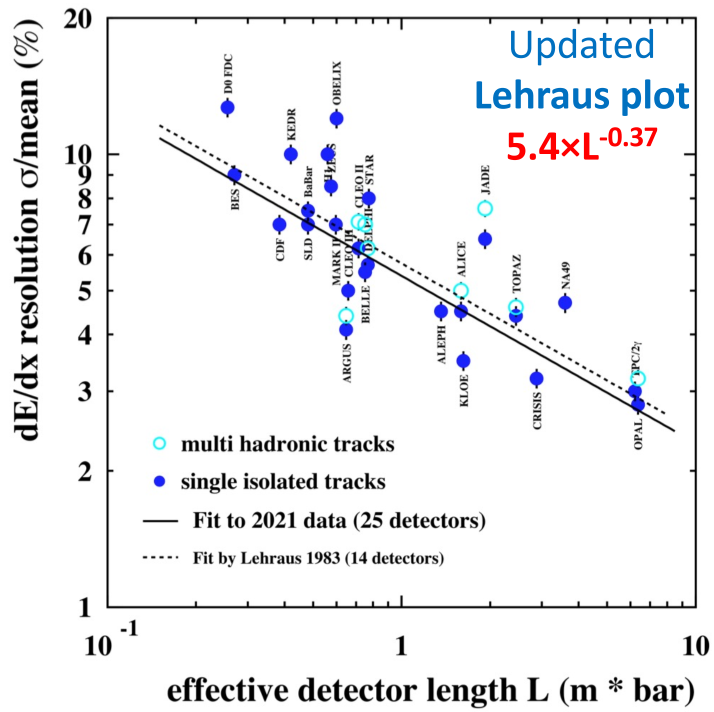

From: Michael Hauschild - RD51 Workshop on Gaseous Detector Contributions to PID – 17 February 2021

PID with dE/dx: general comments

✧Methodology dating back to late ‘70s. Very little progress in performance since then.

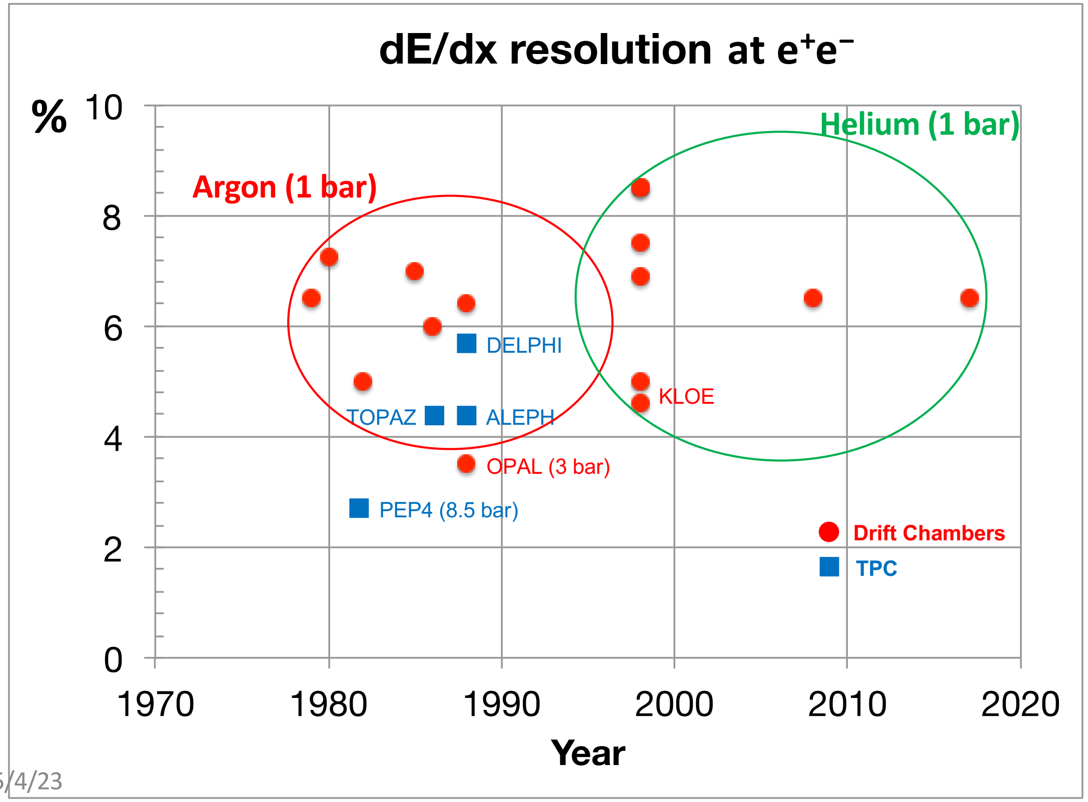

No improvements over >40 years despite:

- Different gases
- Different technologies
- Different geometries

PID with dE/dx: general comments

- ✧Methodology dating back to late ‘70s. Very little progress in performance since then.
- ✧Using the Allison-Cobb parameterization, a **dE/dx resolution** between **4.0% and 4.5%** is granted for a gaseous detector at **FCC-ee** (is it sufficient?)
- ✧An **increase in pressure at 2 bar** improves the resolution **by 20%** without jeopardizing too much the momentum resolution (tanks to the very low He density, if it can be used).
- ✧A further **25%** improvement may come at the expensive cost (in terms of money and stability) of a **finer (×2) drift cell granularity.**
- ✧New techniques (**ML**?) might mark the difference with respect to **maximum likelihood** and/or **truncated mean** methods (but do not expect miracles).
- ✧Only a completely different approach, like **cluster counting**, will provide a significant step forward.

Cluster counting/timing (CC/T)

The number of primary ions N_{cl} created along the trajectory of a charged particle is distributed according to **Poisson statistics**, as opposed to the total number of ions, proportional to the total energy deposited by ionization, which follows a **long-tailed distribution**.

Advantages of dN_{cl}/dx over dE/dx

N_{cl} number of primary ionizations

- independent from **cluster size fluctuations**
- insensitive to **highly ionizing δ-rays**
- independent from **gas gain fluctuations**
- independent from **electronics gain** (calibration)
- a 2 m track in a He – mix gives **N_{cl} > 2400 (for a m.i.p.)**:

  $\sigma_{dNcl/dx} / (dN_{cl}/dx) = N_{cl}^{-1/2} < 2.0\%$

  (at 100% counting efficiency)
- a **factor > 2 better** than **dE/dx**
- resolution scales with $L^{-0.5}$ (not $L^{-0.37}$ as in dE/dx)

Advantages of Helium over Argon

- lower **primary ionization density** (1/5)
  → larger spatial separation
- lower **drift velocity** (1/2)
  → larger time separation
- lower average **cluster size**
- lower **singe electron diffusion**

Recipe in time domain

Front end bandwidth (≈ 1 GHz)
Sampling > 2 GSa/s, ≥ 12 bit
S/N ratio > 8

Recipe in space domain

High readout granularity
High spatial resolution
Very low transverse diffusion

Cluster counting: not a new idea!

Wilson chambers (30's)

E. J. Williams and F. R. Terroux - *Proc. R. Soc. A 1930 126*

Observations.—Every ion produced in the cloud chamber acts as a nucleus for the condensation of water and can be recorded on a photograph. A primary ion may be accompanied by a number of secondary electrons so that the track of a β-particle consists of clusters of ions, each cluster signifying the production of one primary ion. The measurement of the primary ionisation therefore consists of counting the numbers of clusters or groups produced by a β-particle in a given distance. The size of the clusters depends on the diffusion of the secondary ions and this depends on the nature and density of the gas in the chamber. In the present experiments the gases in the chamber

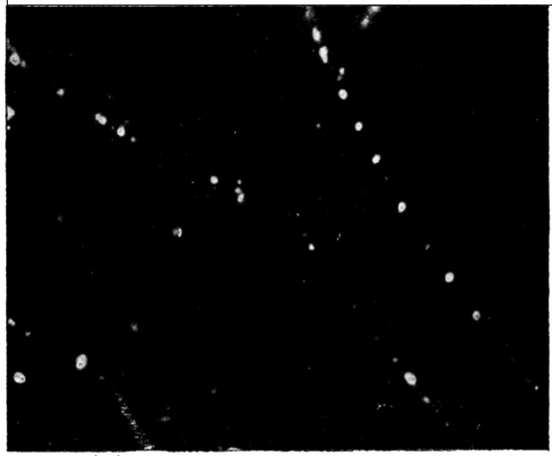

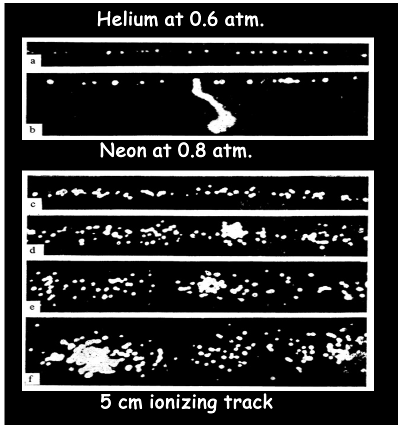

Streamer chambers (60's)

V. A. Davidenko, B. A. Dolgoshein, V. K. Semenov and S. V. Somov, *Nucl.Instrum.Meth. 67 (1969) 325*

Low efficiency G-M (40's)

F L Hereford, *Phys. Rev. 72, 982 (1947)*

The method employed in the determination of the primary ionization in hydrogen utilizes the dependence of the efficiency of a Geiger counter upon the primary ionization. This dependence is as follows:

$$\text{Eff.} = 1 - e^{-lJp}. \qquad (3)$$

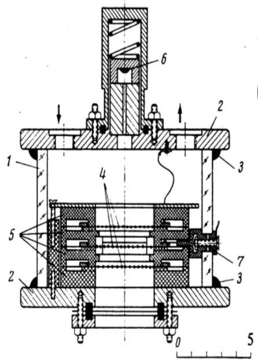

Spark chambers (70's)

V. S. Asokov, G. I. Merzon et *al.* *Sov. Phys. JETP 46(1), July 1977*

FIG. 1. Construction of the low pressure spark chamber: 1—glass case, 2—chamber cover, 3—vacuum cement, 4—wire electrodes, 5—teflon rings, 6—radioactive source (Sr_{38}^{90}), 7—high-voltage lead.

Cluster counting: not a new idea!

Time Expansion Chamber (late 70's)

A. H. Walenta, A.H. *IEEE Trans.Nucl.Sci. 26 (1979) 73-80*

(time domain)

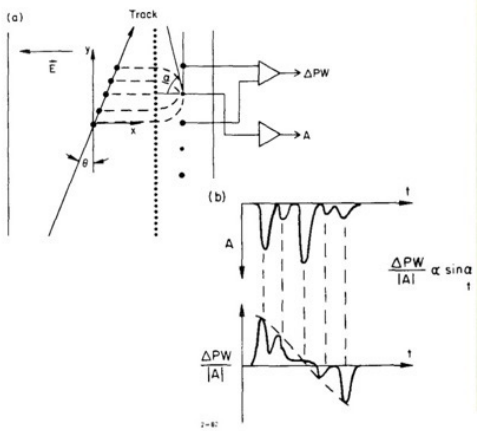

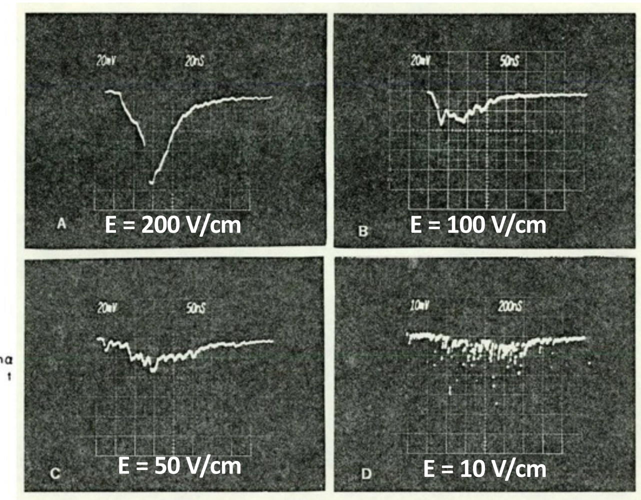

gas: pure Isobutane at

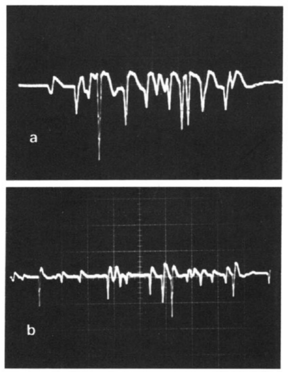

Fig. 10. Individual clusters obtained from a LPMSC irradiated with β particles from a ^{90}Sr source, in the direction parallel to the drift field (longitudinal drift mode). The individual clusters are well separated. (a) Drift field $E/p = 0.6$ V/cm Torr, 0.5 μs and 50 mV/div. (b) $E/p = 0.3$ V/cm Torr, 1 μs and 50 mV/div. Pure isobutane, 20 Torr. Conversion gap length: 60 mm

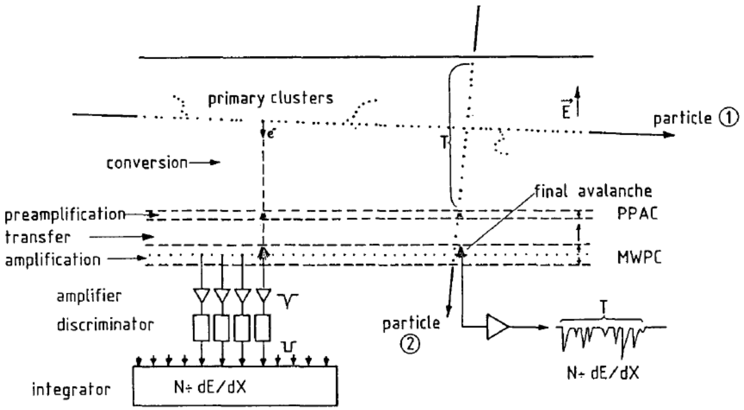

Low-pressure multistep avalanche chambers (late 80's)

A. Breskin and R. Chechik, *Nucl.Instrum.Meth. A252 (1986) 488-49*

(space domain)

PID with dN_{cl}/dx in the time domain: the task

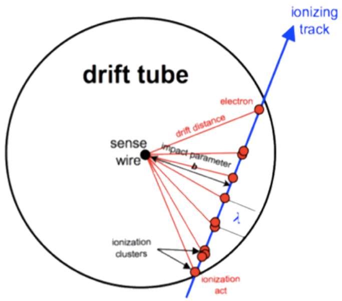

Determine, in the signal, the **ordered sequence of the electron arrival times**:

$$\{t_j^{el}\} \qquad j = 1, n_{el}$$

Based on the dependence of **the average time separation between consecutive clusters** and on the **time spread due to diffusion**, as a function of the drift time, **define** the **probability function**, that the ***j***th **electron** belongs to the ***i***th **cluster**:

$$P(j,i) \qquad j = 1, n_{el}, \quad i = 1, n_{cl}$$

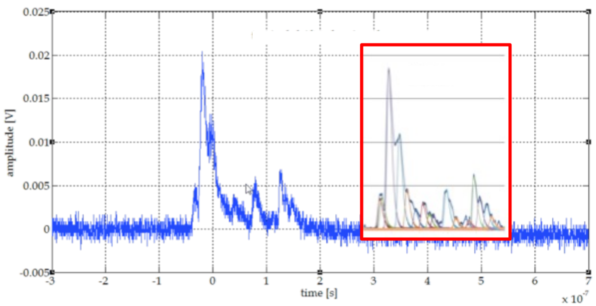

from this **derive** the most probable **time ordered sequence of the original ionization clusters**:

$$\{t_i^{cl}\} \qquad i = 1, n_{cl}$$

and the total number of clusters

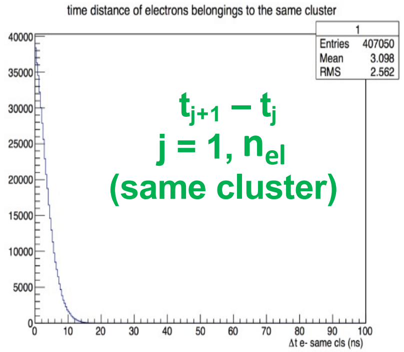

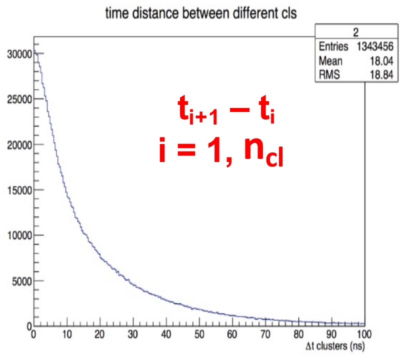

Moreover,
for any given first cluster (**FC**) drift time t_1, the **cluster timing technique** exploits the drift time distribution of all successive clusters to statistically (**MPS**) or using **ML techniques**, determine, hit by hit, the most probable **impact parameter**, thus reducing the **bias** and improving the average **spatial resolution** with respect to that obtainable with the FC method alone:

over a 1 cm drift cell, **spatial resolution** may improve by ≳ 20%
down to ≲ 80 µm.

Fringe benefits of the cluster timing technique are:

- **event time stamping (at the level of ≈ 1 ns);**
- **improvements on charge division;**
- **Improvements on left-right time difference.**

PID with dN_{cl}/dx in the time domain: simulations

200 × 1 cm samples in 90/10 He/iC_4H_{10}

full simulation

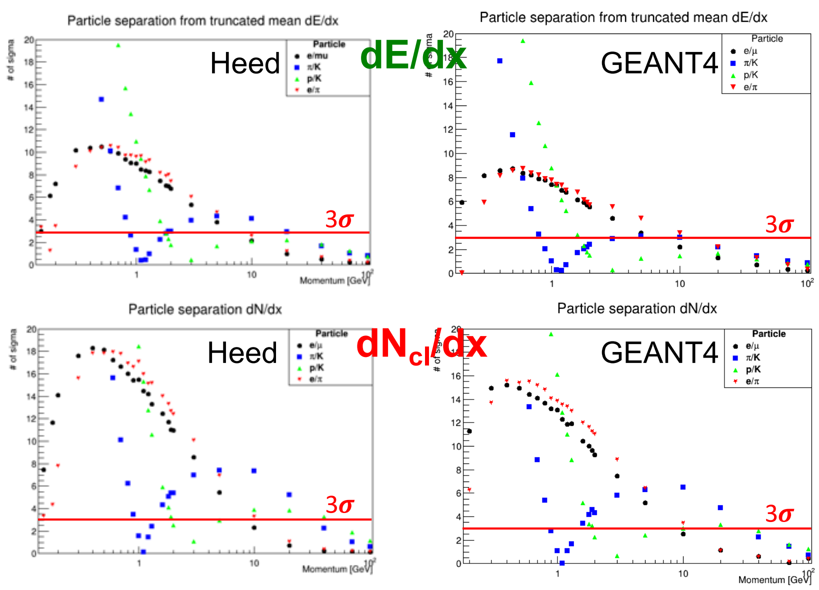

F. Cuna, N. De Filippis, F. Grancagnolo, G. Tassielli, *Simulation of particle identification with the cluster counting technique*, arXiv:2105.07064v1 [physics.ins-det] 14 May 2021

Geant4 uses the cluster density and the cluster size distributions derived from **Heed**, however, they **disagree**, most likely, due to a different choice of the E_{cut} parameter (the maximum energy of an electron still associated to a track in the simulation)

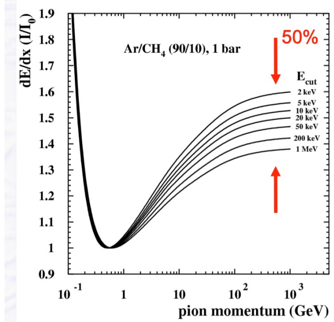

From: Michael Hauschild – *op. cit.*

IDEA drift chamber
expected π/K separation

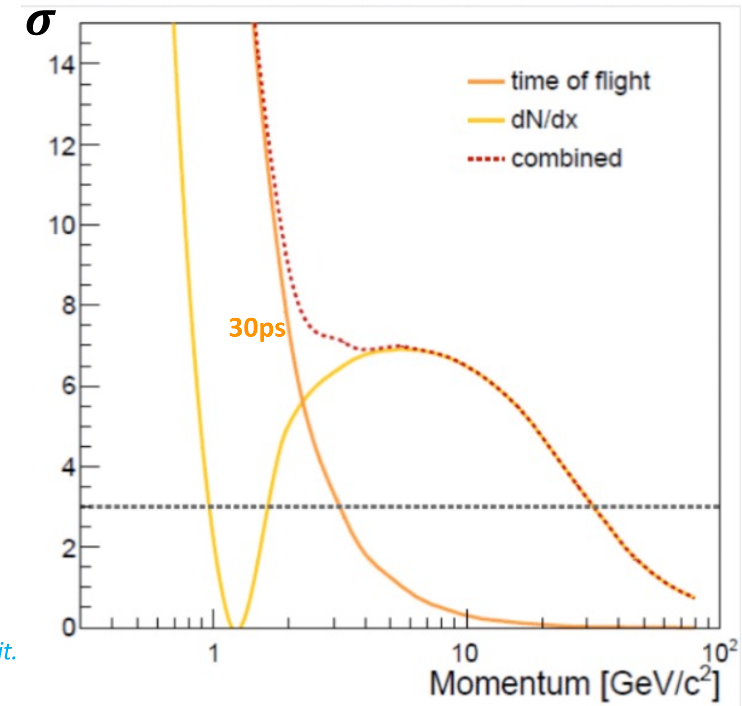

PID with dN_{cl}/dx in the time domain: measurements

IDEA test prototypes (square drift tubes)

- Beam test at CERN-H8 during 2021 and 2022 with Fermi plateau muons (next beam test at CERN-T10 on muons relativistic rise, next month
- Simulations trained on data
- Peak finding algorithms trained on simulations

Derivative method

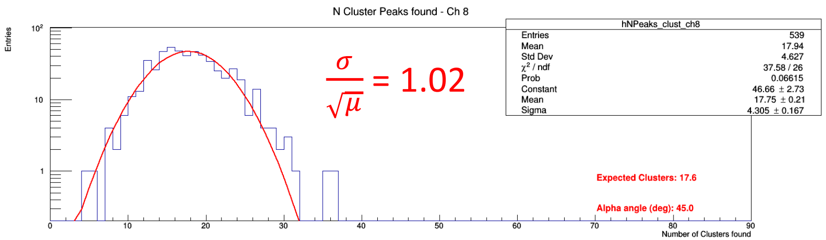

Running template method

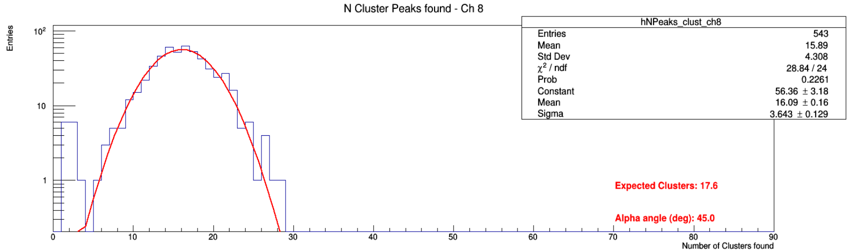

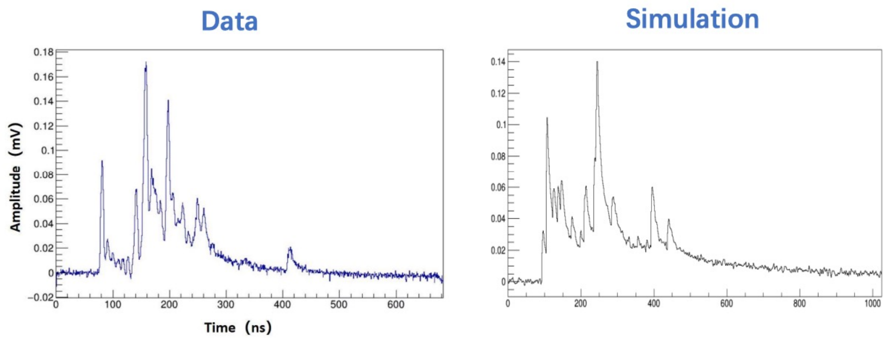

Machine Learning

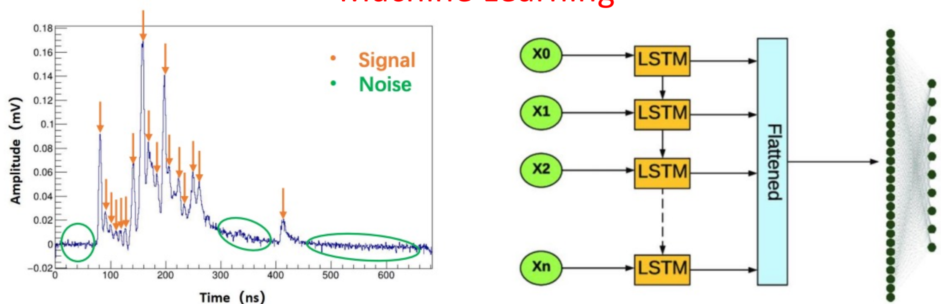

From Guang Zhao - IHEP

PID with dN_{cl}/dx in the space domain: the task

Most promising configuration for separating ionizazion clusters in space is a **TPC** instrumented with micro pattern devices (**multi-GEMs with pad readout** or **TimePix** and **MicroMegas with TimePix**)

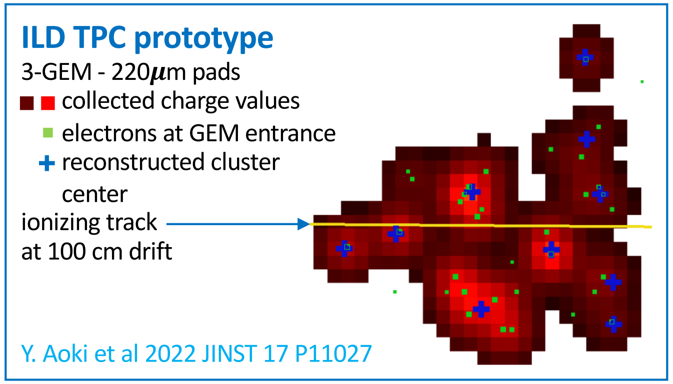

Y. Aoki et al 2022 JINST 17 P11027

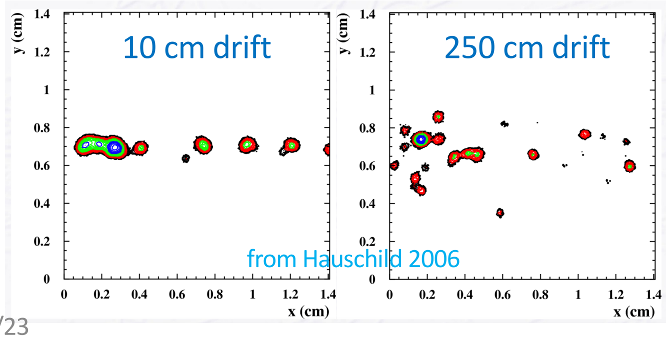

from Hauschild 2006

which granularity is needed?

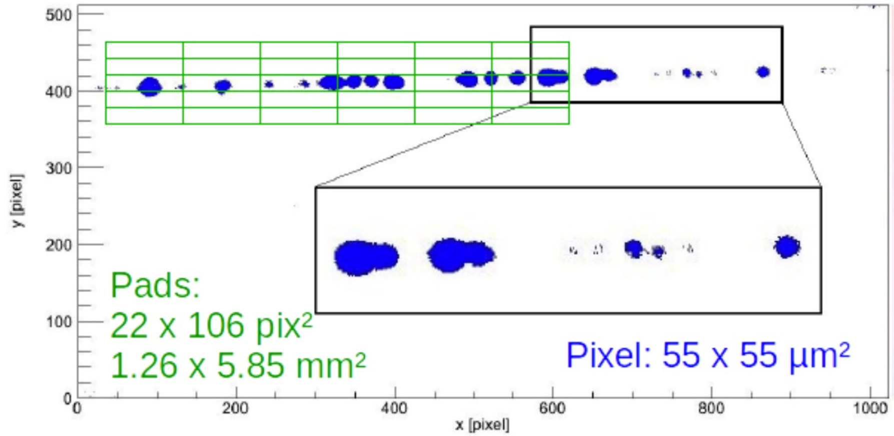

TimePix Octoboard readout

Ulrich Einhaus, Jochen Kaminksi and Michele Caselle
A TPC readout with GEMs, pads and Timepix
arXiv:1801.07178v1 [physics.ins-det] 19 Jan 2018

PID with dN_{cl}/dx in the space domain: performance

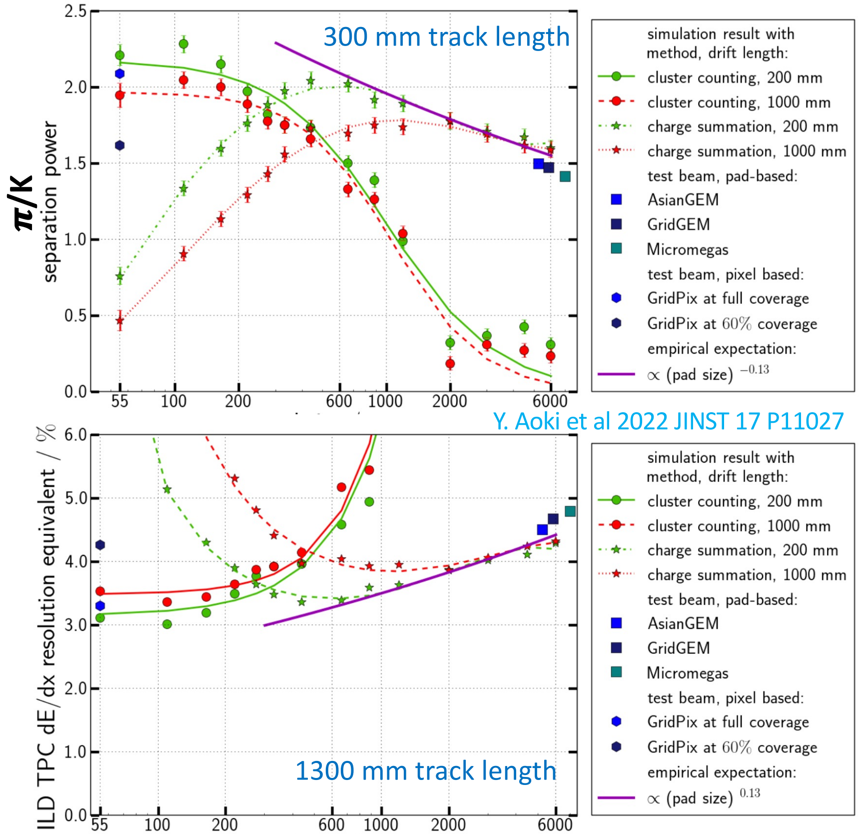

Y. Aoki et al 2022 JINST 17 P11027

Conclusions by Ulrich Einhaus at the 4th FCC Physics and Experiments Workshop, 12.11.2020

- Pad-based TPC readout structures with 6 mm granularity achieve the ILD target dE/dx resolution of 5 % (or better).
- Pixelised readout with a 55 µm granularity achieves a resolution of 3.5 % with dE/dx, and of 3.3 % if combined with cluster counting. → This should improve in future analyses!
- Simulation shows: the higher the granularity, the better the performance. Cluster counting kicks in at the pixel level O(200µm).
- PID can contribute to high level reconstruction and a large number of physics analyses, and clear dependencies on the PID performance can be observed.

CONCLUSIONS

- A clear set of **requirements** for **PID** must be established by defining some benchmark physics channels and by stating their relative **performance goals**.
- As far as gaseous detectors are concerned, PID is intrinsically related to tracking and constitutes a valid cheap option, without the need of introducing additional subdetectors.
- The solid traditions of the charge integration (**dE/dx**) technique guarantees a resolution below **5%**. Small improvements are possible to a very limited extent, given the intrinsic fluctuations of the process. **But is 5% sufficient?**
- **Cluster counting represents the step forward**: a **2.5%** resolution is at reach when applied in the **time domain** (from **IDEA beam tests**) and **3.3%** has already been demonstrated (from **ILD TPC studies**) in the **space domain**.
- More progress to come!

Spares

$\phi \rightarrow K^+K^-$
LHCb RICH

(preliminary data at
900 GeV p–p collisions)

all combinations of pairs of tracks without PID

tracks identified as kaons with RICH

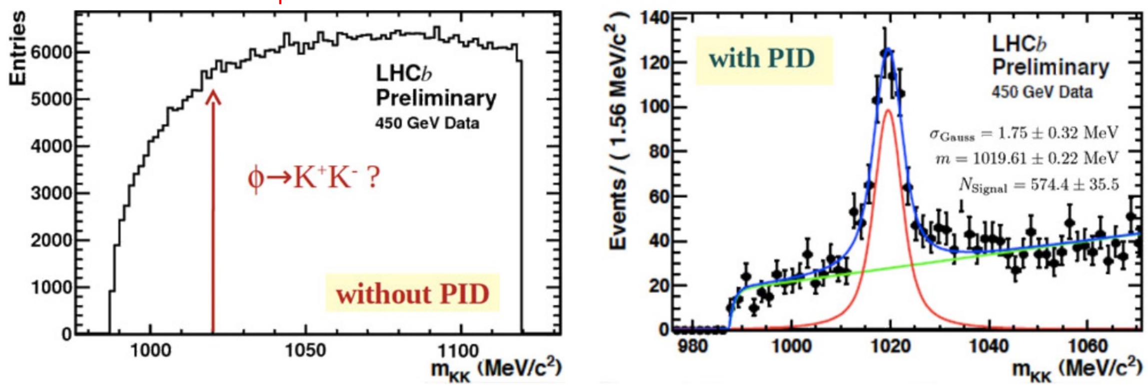

From: Christian Lippmann - *Particle identification* - arXiv:1101.3276v4 [hep-ex] 12 Jun 2011

PId with dE/dx: the straggling function

comparison with data

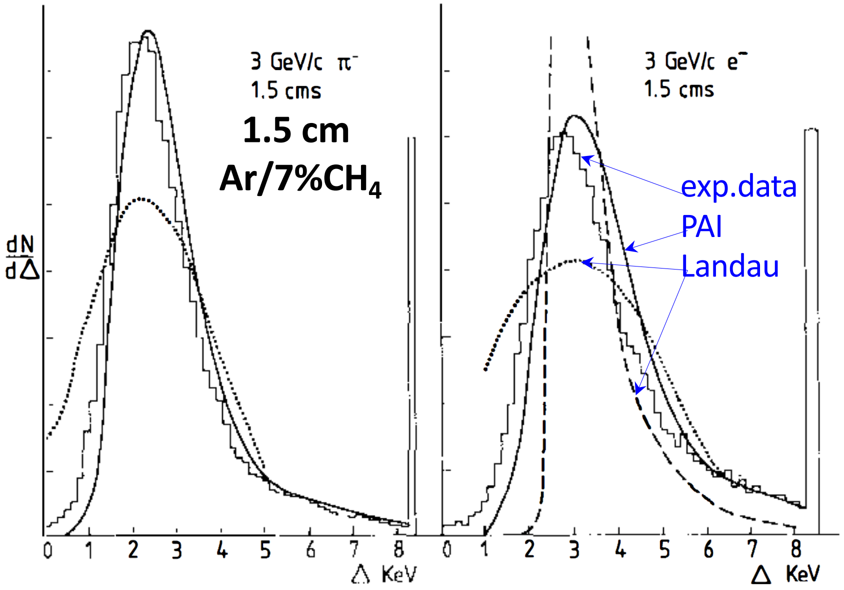

Figure 9 Experimental energy-loss distributions of Harris et al (1973) for π and e at 3 GeV/c in 1.5 cm of argon/7% CH_4 at normal density. The dashed and dotted curves are calculations using the model of Landau (1944) with corrections of Maccabee & Papworth (1969) and Blunck & Leisegang (1950) respectively. The solid curves are the predictions of the PAI model.

W. Allison and J. Cobb
Relativistic charged particles identification by energy loss
Ann. Rev. Nucl. Part. Sci. 1980. 30: 253-98

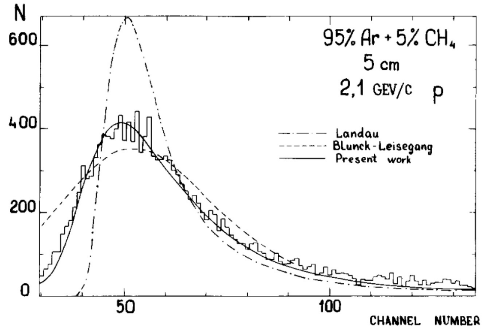

Fig. 4. The energy loss distributions for 2.1 GeV/c protons (near ionization minimum) in 5 cm of a mixture of Ar (95%) and CH_4 (5%). The histogram is obtained in the experiment by Kopot et al.[13]. The smooth curves are calculated for 5 cm of Ar at NTP without correction for detector resolution. The dash–dotted, dashed and solid curves are Landau, Blunck–Leisegang distributions and present work results respectively. Experimental and calculated data are normalised to the same Δ_{mp}.

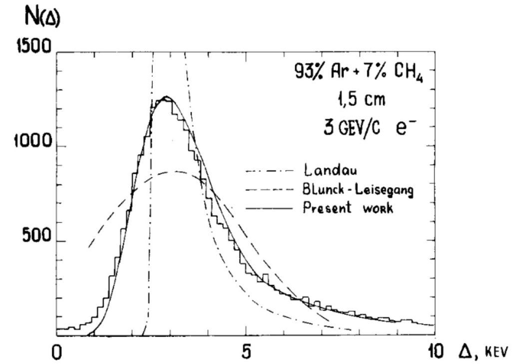

Fig. 5. The energy loss distribution for 3 GeV/c electrons (Fermi plateau region) in 1.5 cm of a mixture of Ar (93%) and CH_4(7%). The histogram is taken from a paper by Harris et al.[9]. The smooth curves are calculated for 1.5 cm of Ar at NTP without correction for detector resolution. The dash-dotted, dashed and solid curves are Landau, Blunck–Leisegang predictions and present work results respectively.

V. Ermilova, L. Kotenko, G. Merzon
Fluctuations and the most probable values of relativistic charged particle energy loss in thin gas layers
NIM 145 (1977) 555

✧ Number of electrons generated per cluster subject to large fluctuations

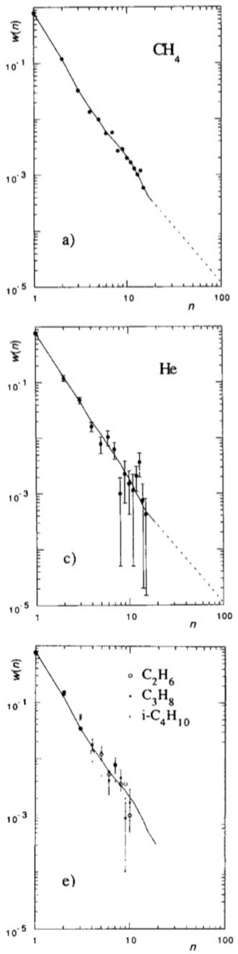

H. Fischle, J. Heintze and B. Schmidt,
Experimental determination of ionization cluster size distributions in counting gases,
NIM A 301 (1991)

k	CH_4	Ar	He	CO_2
1	78.6	65.6	76.60	72.50
2	12.0	15.0	12.50	14.00
3	3.4	6.4	4.60	4.20
4	1.6	3.5	2.0	2.20
5	0.95	2.25	1.2	1.40
6	0.60	1.55	0.75	1.00
7	0.44	1.05	0.50	0.75
8	0.34	0.81	0.36	0.55
9	0.27	0.61	0.25	0.46
10	0.21	0.49	0.19	0.38
11	0.17	0.39	0.14	0.34
12	0.13	0.30	0.10	0.28
13	0.10	0.25	0.08	0.24
14	0.08	0.20	0.06	0.20
15	0.06	0.16	0.048	0.16
16	(0.050)	0.12	(0.043)	0.12
17	(0.042)	0.095	(0.038)	0.09
18	(0.037)	0.075	(0.034)	(0.064)
19	(0.033)	(0.063)	(0.030)	(0.048)
≥20	$(11.9/k^2)$	$(21.6/k^2)$	$(10.9/k^2)$	$(14.9/k^2)$

HEED simulation
1 cm
He/iC_4H_{10} - 90/10

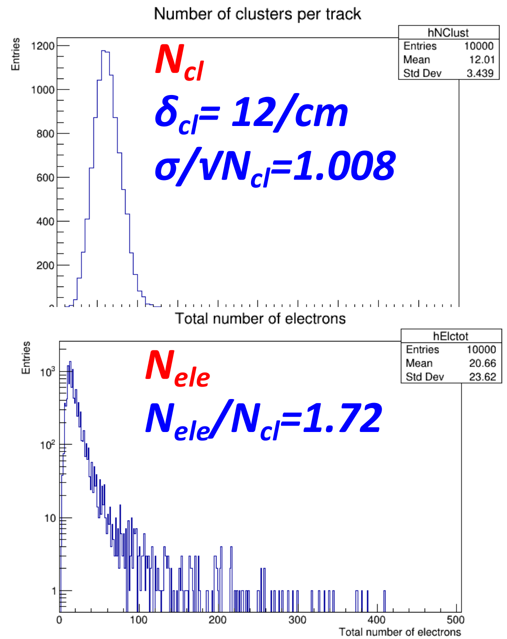

F. Cuna, G. Tassielli
private communication

notice the steeper distribution for **He** with respect to **Ar**

✧ Parameterization of resolution $\sigma(\lambda_0)$

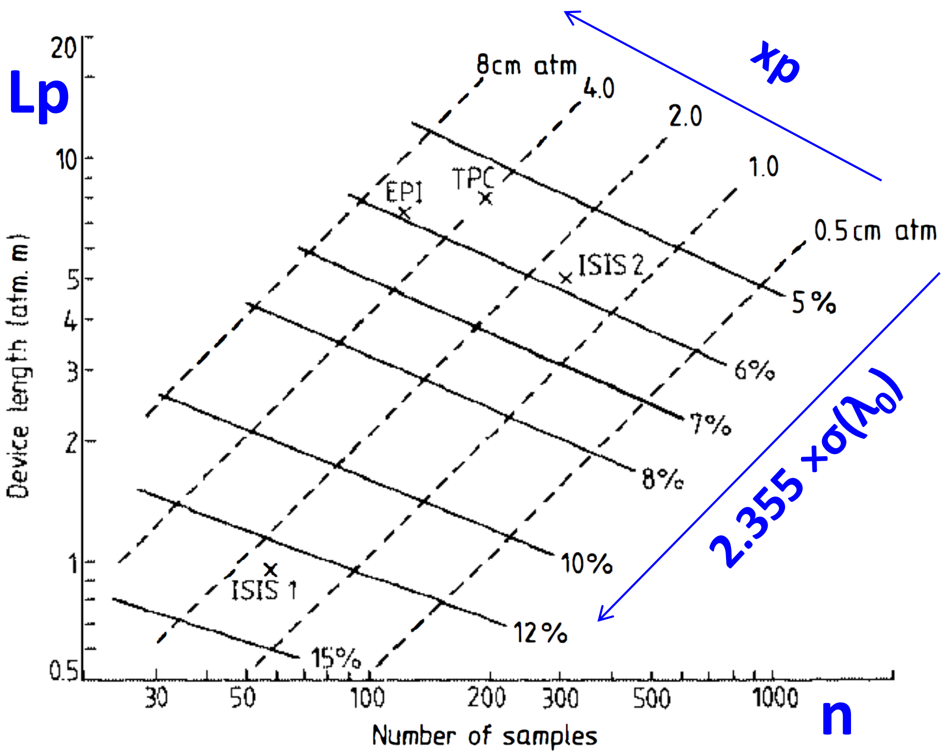

W. Allison and J. Cobb
Relativistic charged particles identification by energy loss
Ann. Rev. Nucl. Part. Sci. 1980. 30: 253-98

- keeping x fixed and increasing n or L improves the resolution
- keeping n fixed and varying L and x improves the resolution (slide)
- what is the optimal sample length for a fixed total length L?

  the finer the better **($n^{-0.14}$)**

ALEPH

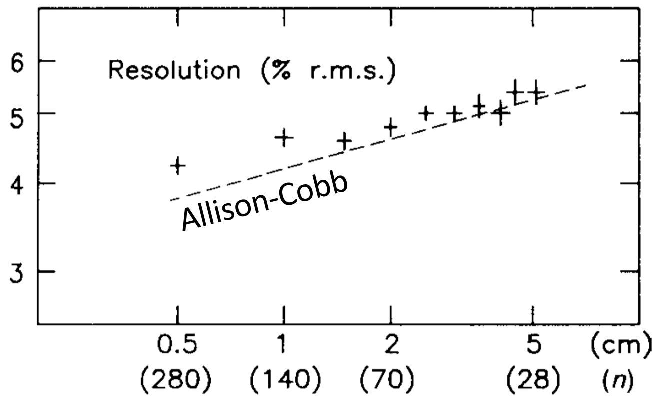

✧ **Average number of electrons per cluster increases with sample length**

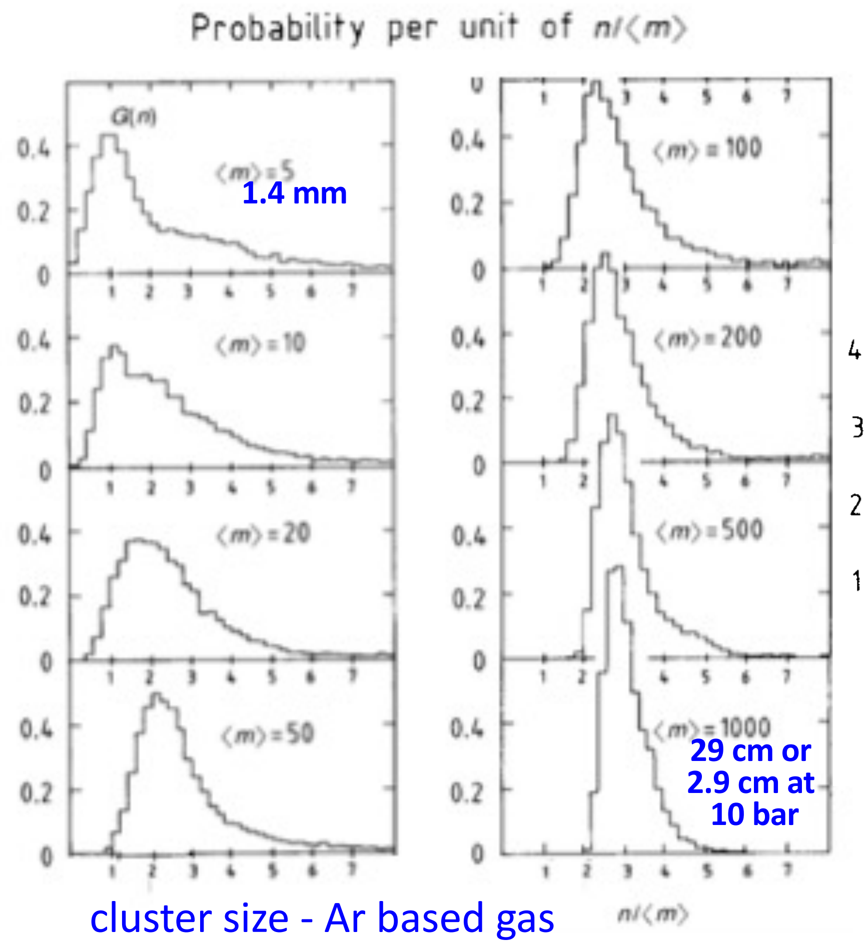

cluster size - Ar based gas

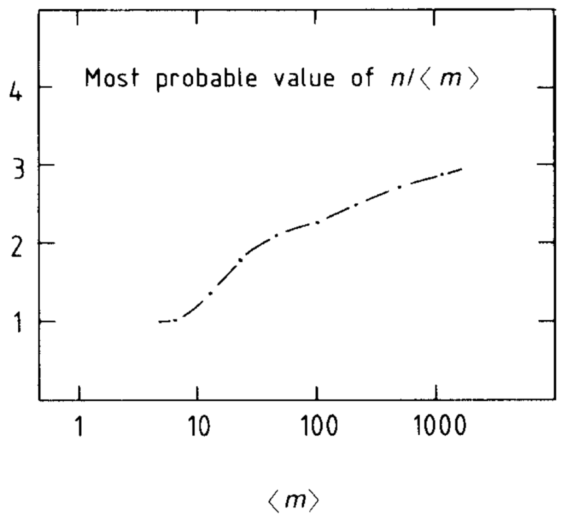

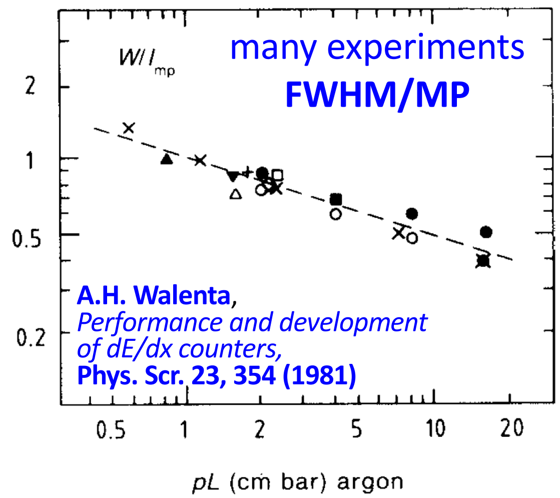

PId with dE/dx: gas choice

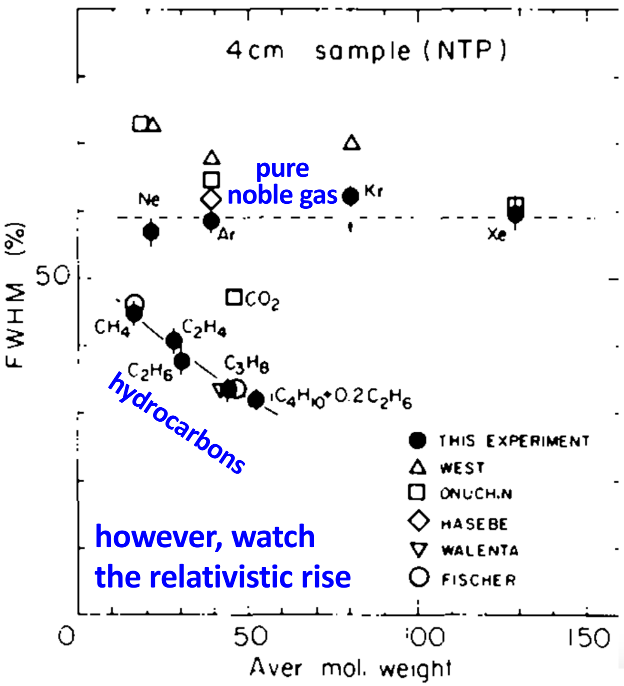

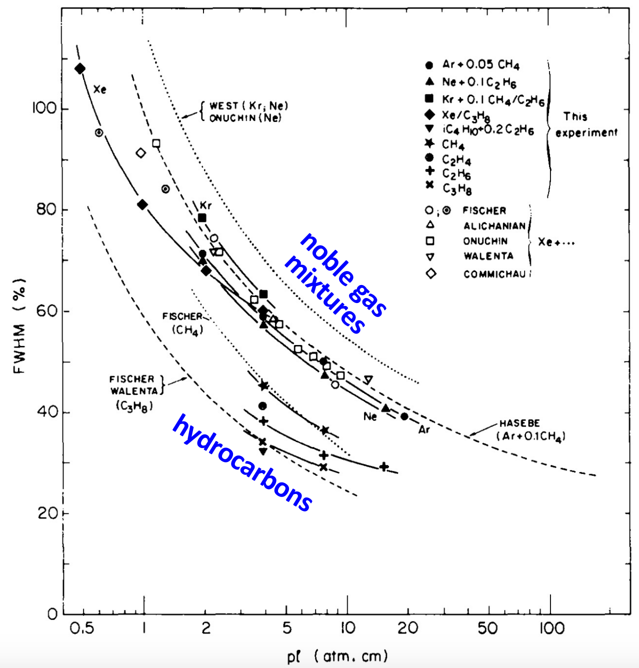

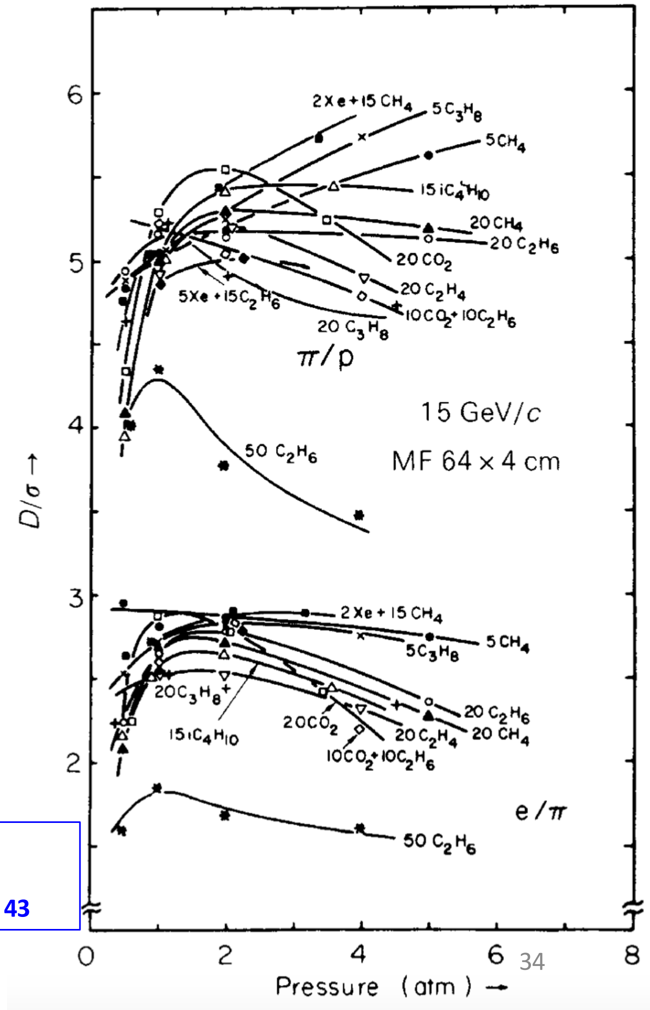

I. Lehraus, R. Mattewson and W. Tejesse, *dE/dx measurements in Ne, Ar, Kr, Xe and pure hydrocarbons,* **NIM 200 (1982) 199**

I. Lehraus, *Progress in particle identification by ionization sampling,* **NIM 217 (1983) 43**